Journal of Advanced Research in Natural and Applied Sciences
dergipark.org.tr/en/pub/jarnas
Open Access

ISSN: 2757-5195 | 11 (3) (2025) 286-296 | doi.org/10.28979/jarnas.1707918

The Grindability and Optical Properties of Glass-Ceramic Frits for Inkjet Printing

Damla Yazıcı[1], Berkay Yazırlı[2], Kağan Kayacı[3], Alpagut Kara[4]

Article Info
Received: 10 Jun 2025
Accepted: 29 Aug 2025
Published: 30 Sep 2025
Research Article

Abstract − Decoration is the most critical feature in determining the final quality of ceramic tiles. Traditional decoration techniques, such as screen printing and rotocolor, have been transitioned to inkjet printing due to technological improvements in the ceramic industry. Inkjet technology has enabled an unlimited variety of decorative designs, facilitated the efficient storage of designs, and made it possible to apply decoration without direct contact with the product. Additionally, inkjet decoration enhances the natural appearance of the image. Inkjet printers use inks in which inorganic particles are suspended in a carrier medium. Recently, effect materials that provide surface properties such as matte and gloss have also been utilized. The prepared effect material exhibits an average particle size (d_{50}) of 0.3-0.6 µm, which is required to prevent clogging of the nozzle head in the inkjet printer. Effect materials are needed to demonstrate optimum viscosity, density, and particle size distribution, ensuring their suitability for use in inkjet printers. This study examines the particle size distribution, milling behavior, rheological properties, and morphological characteristics (as observed by SEM) of transparent, opaque, and matte glass-ceramic frits used in wall and floor tiles. Furthermore, optical properties were measured using gloss meters and colorimetric devices. The results demonstrate that the investigated frits fulfill the particle size and rheological requirements for jetting in inkjet printers, achieving d_{90} values below 1 µm to prevent nozzle clogging and post-dilution viscosities within the ideal range of 15–25 mPa·s. The frits were determined to be suitable for application on wall and floor tiles.

Keywords − *Grinding, particle size, optical properties, color, gloss*

1. Introduction

Decoration is an essential aspect of the ceramic tile industry. The process is continually improving, with an increasing emphasis on aesthetic appearance and personal preferences [1]. The flat screen-printing method, which began in 1960, was replaced by rotary screen printing in 1970, and later by gravure printing in 1990 [2]. Inkjet technology has been adopted in the ceramic tile industry and has progressively become the most widely utilized technique in ceramic decoration since the 2000s. Efficient ink usage, non-contact decoration, and easy pattern changes have become possible with the transition from traditional methods to inkjet technology. In addition, this technology offers several advantages, including an unlimited variety of decorations, easy storage of designs, and the ability to apply them to uneven surfaces [3, 4].

[1]damlayazici@kale.com.tr (Corresponding Author); [2]berkayyazirli@kale.com.tr; [3]kagankayaci@kale.com.tr;
[4]alpagut.kara@sabanciuniv.edu
[1,2,3]Kaleseramik Research-Development Center, Çan, Çanakkale, Türkiye
[1,4]Department of Materials Science and Engineering, Faculty of Engineering, Eskişehir Technical University, Eskişehir, Türkiye
[4]Sabancı University Nanotechnology Research and Application Center (SUNUM), Sabancı University, İstanbul, Türkiye

Two different mechanisms are used in inkjet technology: Continuous inkjet (CIJ) and drop-on-demand (DOD). DOD mechanism is utilized, where ink droplets are transferred from the print head to the surface in ceramic tile decoration [5, 6]. Ink ejection in the DOD mechanism is achieved by generating pressure waves through the deformation of a piezoelectric actuator under an electric field [7]. Inks used in inkjet printers generally consist of inorganic pigments, a solvent, and a dispersant. Ceramic inorganic pigments used as colorants are milled to form a suspension in a low-viscosity organic solvent. The dispersant prevents the agglomeration of pigment particles [8]. Inkjet inks require some physical properties such as particle size distribution, viscosity, and density [9]. Ink solutions are formulated to enable inkjet printing, taking into account defined printing parameters, rheological behavior, stability, and surface properties [7]. The particle size of the ink composition is reduced to submicron size to prevent clogging of inkjet printer printheads [10]. The micronization process, performed in high-energy ball mills using Y-stabilized zirconia beads, produces pigments with a median particle size typically ranging from 0.3 to 0.6 μm [11]. The standard four pigment cyan, magenta, yellow, and black (CMYK) are utilized in inkjet printing, and glass frit suspension is also applicable in this printing [12]. Glazes are composed of raw materials such as quartz, alumina, feldspar, calcite, magnesite, and frit, which contribute to both the surface properties and the decorative aesthetic of ceramic bodies [13, 14]. Frits are produced by melting a mixture containing glass-forming components, such as silica, and alkali oxides at approximately 1500°C, followed by rapid cooling in water, to obtain non-uniform glass particles [15].

Frits with distinct characteristics such as opacity, gloss, fusibility, and viscosity are available. Transparent glazes, typically obtained from frits that remain uncrystallized during firing and which exhibit low abrasion resistance, are characterized by light transmission without scattering [16-18]. Opaque glazes contain zircon, and their opacity is related to the refractive index. The difference in refractive index between the opacifier and the glassy matrix increases light scattering, thereby enhancing the opacity of the glaze [16]. On the other hand, the high surface roughness causes the incident light to reflect diffusely in matte glazes. As a result, the intensity of the reflected light decreases, reducing the gloss value [19]. The pigments used in inkjet printing provide coloration; however, different optical and textural properties, such as transparency, opacity, or a matte surface finish, are achieved through the application of effect materials.

Numerous studies in the relevant literature have explored the applications of inkjet technology in the ceramic tile industry. Among these studies, the use of ceramic pigments in inkjet inks is included. In addition, developments and challenges in the use of pigments in inkjet technology have been discussed [4, 10]. The rheological behavior and stabilization of water-based inkjet inks have also been investigated [20]. Moreover, there are studies on the development of inkjet ink formulations and environmentally friendly production methods. However, there is a dearth of literature examining the application of glass ceramic frits as effect materials on ceramic tile surfaces using inkjet printing technology and their effects.

This study aims to investigate the use of glass-ceramic frits as effect materials, which exhibit transparent, opaque, and matte surface appearances after firing in inkjet printers. The evolution of particle size distribution, rheological properties, morphological behavior, and regime differences of glass-ceramic frits applied to wall and floor tiles are discussed in detail. By analyzing these characteristics, the study provides insights into optimizing the performance of effect materials for digital decoration applications in the ceramic industry.

2. Materials and Methods

Three commercial frits (Kale Frit, Türkiye) with different chemical compositions and optical appearances after firing (MAT: matte, OPAK: opaque, and TRS: transparent) were selected for the studies. The chemical analysis of the frits was performed using the X-ray Fluorescence (XRF, Panalytical Axios Max) method (Table 1). To determine the melting behavior of the frits, a heat microscopy device (Misura 3.32 ODHT HSM) was used, with the temperature increasing to 1300°C at a rate of 40°C/min. The linear thermal expansion measurements were carried out using a dilatometer (Netzsch DIL 402) at a heating rate of 10 °C/min. The heat microscopy

results, and linear thermal expansion values of the frits are shown in Table 2. Milling additives and diluent solvents were used as chemical agents during the milling and dilution stages to enhance grinding performance.

The micronization process was carried out in two stages: pre-grinding (Gabrielli, Italy) and high-energy ball mill (Bluenco, Italy). The particle size of the frits with an average diameter ranging from 5 to 10 mm was reduced using pre-grinding. Samples were prepared using 60 (wt.%) frit and 40 (wt.%) ester-based milling solvent for each glass-ceramic frit. In the pre-grinding stage, alumina balls (0.5 mm, 3 kg) were used to wet grind all the frit compositions at 45 rpm for 40 hours. The final particle size of each frit composition was approximately 8 μm (d_{90}). In the second stage of milling, 1 kg of frit solvent mixture was milled in a 3 L high-energy ball mill (Bluenco) at 1350 rpm for up to 28 hours using Y-stabilized zirconia grinding media (0.35-0.45 μm of (d_{50}), 1.2 L). The particle size distribution was measured by laser diffraction (Malvern Mastersizer 2000) to determine the grinding behavior of TRS, OPAK, and MAT frits. The viscosity measurements were carried out using a rheometer (Kinexus, Malvern) at a shear rate of 20 s^{-1} and a temperature of 40°C.

Table 1. Chemical analysis of TRS, OPAK, and MAT frits (wt.%)

Oxides	TRS	OPAK	MAT Frit
SiO_2	60-65	55-60	45-50
Al_2O_3	2-6	2-6	18-23
TiO_2	0-0.5	0-0.5	0-0.5
Fe_2O_3	0-0.3	0-0.3	0-0.3
CaO	10-15	10-15	20-30
MgO	0-3	0-3	7-15
Na_2O	0-2	0-3	-
K_2O	2-5	2-5	-
ZnO	5-13	5-13	-
B_2O_3	0-4	0-4	-
ZrO_2	-	7-12	-

Table 2. Thermal behavior analysis of TRS, OPAK, and MAT frits

Sample	Sintering (°C)	Softening (°C)	Sphere (°C)	Melting (°C)	α_{400} (10^{-6} °C^{-1})
TRS Frit	915	1115	1140	1240	6.0
OPAK Frit	895	1140	1160	1210	6.2
MAT Frit	885	1280	-	1295	6.7

Effect materials were filtered down to 10 μm and 5 μm, respectively, to ensure that no coarse particles were left for inkjet applications. The solid content of the concentrated frit composition was reduced from 60% (wt) to 42% (wt) using an ester-based solvent for inkjet printing. The densities of the concentrated effect material before dilution were 1450 g/L, whereas after dilution, the densities decreased to 1210 g/L. The obtained density is within the suitable range of 1200 to 1400 g/L for application in inkjet printing [21].

Green floor and wall bodies (30x60 cm) were obtained from the Kaleseramik Factory for the application of TRS, OPAK, and MAT effect materials. Each effect material was applied to the green tiles using an inkjet printer (Projecta, G Plotter) at coating weights of 25, 50, and 100 g/m². Wall tiles were fired at 1130 °C for a total kiln cycle time of 49 min, and floor tiles were fired at 1180 °C for a total kiln cycle time of 65 min in industrial roller kilns at the Kaleseramik Factory.

A gloss meter (Zehntner, ZGM 1110) was used to measure the 60° gloss values of the effect materials on the fired tiles. Chromatic coordinates were determined using a spectrophotometer (Konica Minolta Chroma Meter, CR-400). The surface of the effect materials applied to the tile surfaces was examined by scanning electron microscopy (SEM, Tescan Vega) using secondary electron mode, with an accelerating voltage of 15 kV.

3. Results and Discussion

3.1. Milling Behavior

The particle size distribution of TRS, OPAK, and MAT frits after 24 and 40 hours of pre-grinding is presented in Table 3. The maximum particle size (d_{100}) values for TRS, OPAK, and MAT frits after 24 hours of milling were measured as 18.5, 18.7, and 18.3 µm, respectively. The maximum particle size (d_{100}) values decreased to 12.7 µm for TRS, 15.2 µm for OPAK, and 16.3 µm for MAT after 40 hours of milling. The results revealed that the particle sizes of each frit depend on both the grinding time and the type of frit. The TRS frit showed a higher level of grinding efficiency compared to the OPAK frit. In contrast, the MAT frit exhibited minimum efficiency in the pre-grinding stage.

Table 3. Particle size distribution of TRS, OPAK, and MAT frits after pre-milling

Sample	Time (hour)	d_{50} (µm)	d_{90} (µm)	d_{100} (µm)
TRS	24	4.3	9.6	18.5
TRS	40	3	7	12.7
OPAK	24	3.4	9.7	18.7
OPAK	40	2.5	7.6	15.2
MAT	24	2.4	8.3	18.3
MAT	40	2.4	7.7	16.3

Figure 1 illustrates the particle size distribution of TRS effect materials as a function of milling time (0, 2, 4, 8, 16, and 28 hours) using a high-energy ball mill (Bluenco). The graph initially exhibits a bimodal distribution; however, the distribution transitions into a monomodal distribution after 8 hours.

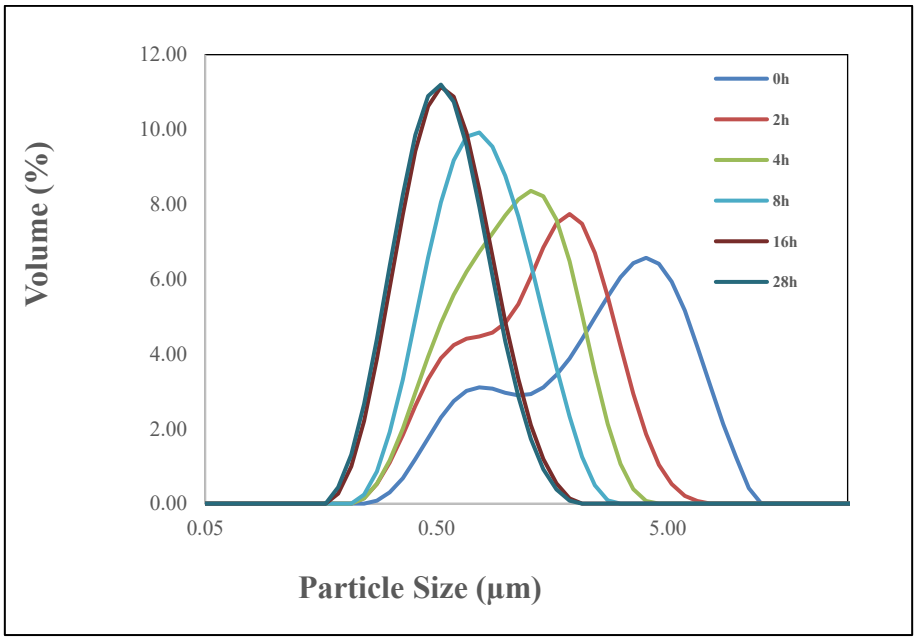

Figure 1. Particle size distribution of effect materials – TRS

In Figure 2, the particle size distribution of the (a) OPAK and (b) MAT effect materials are presented as a function of milling time (0, 2, 4, 8, 16, and 28 hours), which were also performed using a high-energy ball mill (Bluenco). A multimodal distribution was observed initially for the OPAK and MAT effect materials. A bimodal distribution is obtained after 2 hours of milling. However, a stable particle size distribution was achieved after 8 hours. The effect materials exhibit a monomodal distribution and a uniform structure at 28 hours. The observed uniform distribution of particles indicates that the material is suitable for inkjet applications [22]. The analysis of all the effect materials reveals that increasing the milling time results in a monomodal distribution after high-energy ball milling.

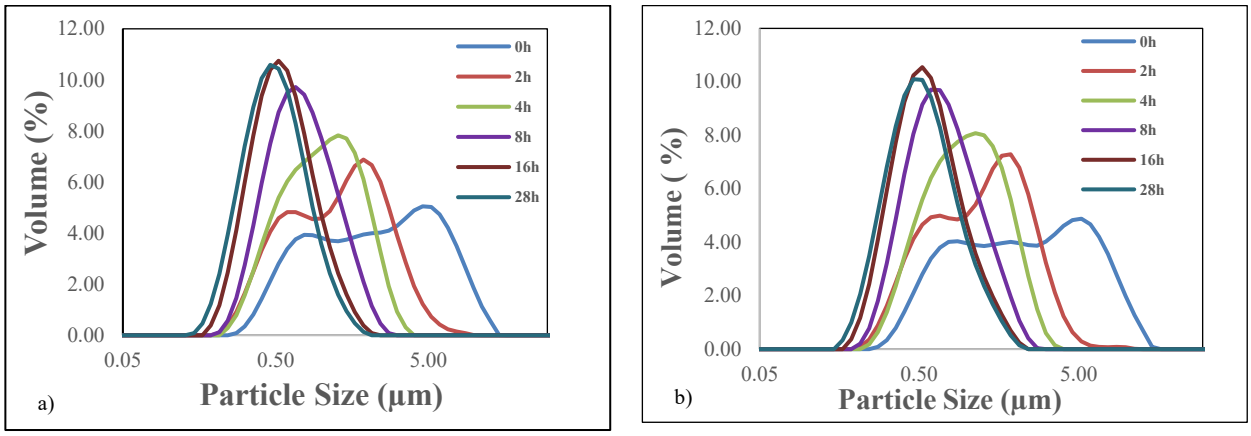

Figure 2. Particle size distribution of effect material (a) OPAK, (b) MAT

Figure 3 presents the particle size at which 90% of the particles are smaller (d_{90}) in the solvent as a function of milling time for TRS, OPAK, and MAT effect materials. The particle size (d_{90}) of each effect material ranges between 0.9 µm and 3.4 µm, depending on the milling time. The particle size decreased to 1.1 µm in the MAT effect material, 1 µm in the OPAK effect material, and 0.9 µm in the TRS effect material for 90% of the particles after 28 hours of milling using high-energy ball milling. Preventing clogging of the nozzles in inkjet printing requires that 99% of the material or pigment particles be smaller than 1 µm [4, 23, 24]. The utilization of high-energy ball milling has enabled the achievement of a particle size suitable for application in the nozzles of the inkjet printing.

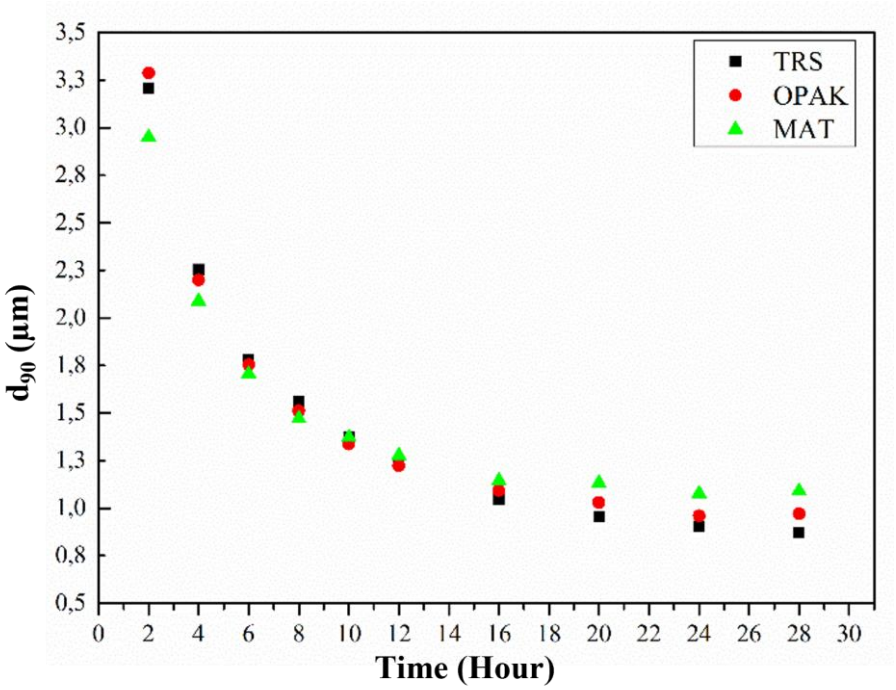

Figure 3. Particle size graph (d_{90}) of TRS, OPAK, and MAT effect materials

3.2. Rheological Behavior

The viscosity variation of the TRS, OPAK, and MAT effect materials at a shear rate of 20 s^{-1} with increasing milling time is presented in Figure 4. The viscosity changes for each material during the high-energy ball milling process exhibit similar behavior up to 12–16 hours. However, a significant increase in viscosity values is observed after 16 hours. This behavior is attributed to the reduction in particle size, which enhances particle interactions. The increased particle interactions lead to a decrease in fluidity [25]. The viscosity values of TRS, OPK, and MAT effect materials were measured after 28 hours of milling as 115.30, 158.70, and 230.80 cP, respectively. The results show that viscosity increases more significantly in the MAT effect material during the high-energy ball milling process. The OPAK and TRS effect materials follow this. MAT frits are typically characterized by crystalline glass systems, which is directly related to their raw material composition. As shown in the chemical analysis (Table 1). MAT frit contains low amounts of the glass former SiO_2, and high concentrations of network modifiers such as CaO and MgO. This oxide distribution reduces the glass-forming ability of the system. The reduction in SiO_2 content leads to a decrease in the glass transition temperature (Tg) [13]. MAT frit exhibited the lowest milling efficiency and the highest viscosity compared to TRS and OPAK frits (Figure 4). This can be correlated with its distinct chemical composition, particularly the higher levels of CaO and MgO (Table 1). Previous studies have similarly reported that frit solubility is strongly affected by the CaO and MgO contents [27]. A high level of CaO and MgO may weaken the effect of the dispersant. This leads to an increase in the viscosity of concentrated ink, and the higher viscosity reduces milling efficiency.

The post-dilution viscosities of the TRS, OPK, and MAT effect materials were measured as 22.57 cP for TRS, 23.96 cP for OPK, and 24.73 cP for MAT. The ideal viscosity range of 15 to 25 mPa.s, required for application in the inkjet printing, was obtained for each effect material with the dilution process [28]. The average particle size (d_{50}) required to prevent clogging of the nozzle head in the inkjet printer is defined as 0.2-0.6 µm [29]. The average particle size (d_{50}) was measured as 0.500 µm for TRS, 0.518 µm for OPAK, and 0.545 µm for MAT effect materials after 28 hours of milling. These results indicate that suitable parameters for inkjet printing were achieved.

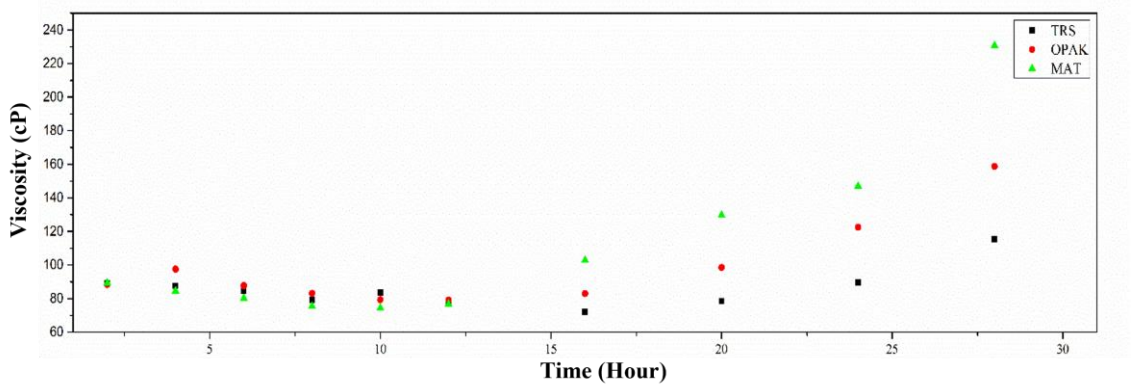

Figure 4. Viscosity (cP) at shear rate of 20 s^{-1} for TRS, OPAK, and MAT effect materials

3.3. Microstructural (SEM) Analysis

In Figure 5, secondary electron images obtained after the application of the TRS effect material on the wall tile and floor tile were presented with distinct surface roughness on the wall tile compared to the floor tile Figures 5a and 5b. The difference in firing temperatures between the floor tile and the wall tile was identified as the determining factor. Floor tile firing temperatures are higher than those of wall tile, and firing times are longer. The viscosity of the melt decreases with increasing temperature, resulting in improved spreading on the surface of the floor tile (Figure 5b).

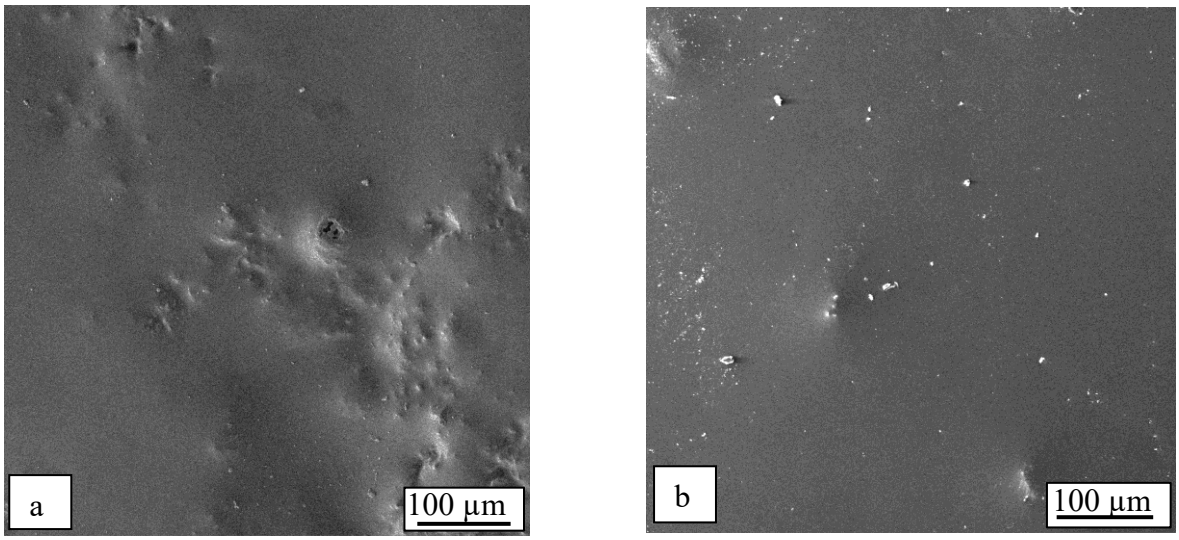

Figure 5. Secondary electron images of TRS effect material: a) Wall tile, b) Floor tile

SEM images of the OPAK effect material applied on the wall tile and floor tile are given in Figure 6. The images revealed variations in surface roughness between the applications on wall tiles and floor tiles in Figures 6a and 6b. The increase in temperature was identified as the factor enhancing the spreading of the material on the surface, as observed in the case of the TRS effect material. However, when the surfaces with TRS and OPAK effect materials are compared, it is observed that the TRS effect material spreads more evenly after firing, both on the wall and floor tiles in Figures 5 and 6. This is due to the difference between the softening temperatures (Table 2) of the frits, and the softening temperature of TRS frits is lower than that of OPAK frits.

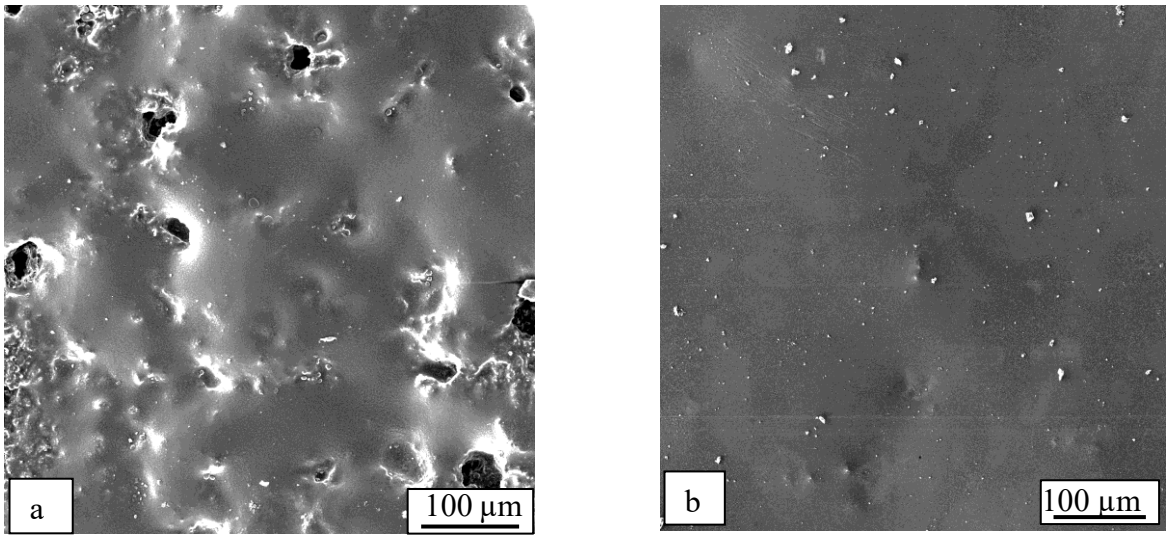

Figure 6. Secondary electron images of OPAK effect material: a) Wall tile, b) Floor tile

The electron microscope images of the sample obtained from the MAT effect material are presented, with applications to the wall and floor tile bodies in Figures 7a–b and 8a–b. The secondary electron images of the matte effect materials show the existence of unmelted particles with sizes ranging from 1 to 2 µm. The lower magnification image of the wall tile application shows fewer topographical differences than the TRS and OPAK effect materials, while high topographic difference is observed over a large planar distance in the floor tile (Figures 7a and 7b). In higher magnification images, particles were not fully sintered, and both wall and floor tile samples contained fine particles (Figures 8a and 8b). This is due to the high softening temperature of the MAT frit (Table 2). The viscosity of the melt does not decrease, and the viscous flow is slow due to insufficient temperature.

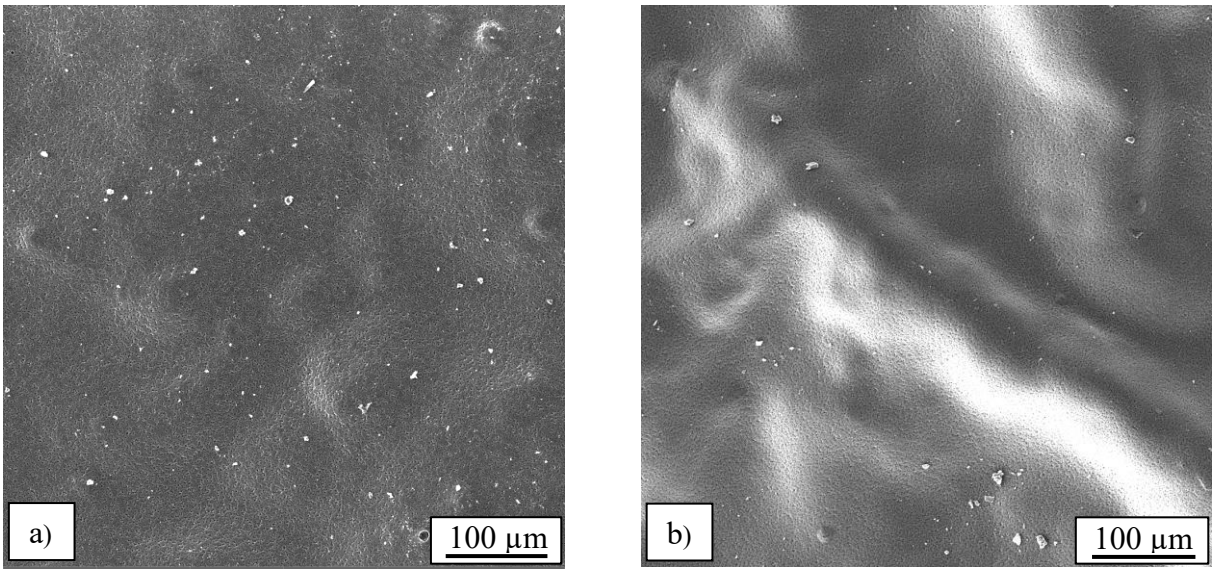

Figure 7. Secondary electron images of MAT effect material: a) Wall tile, b) Floor tile

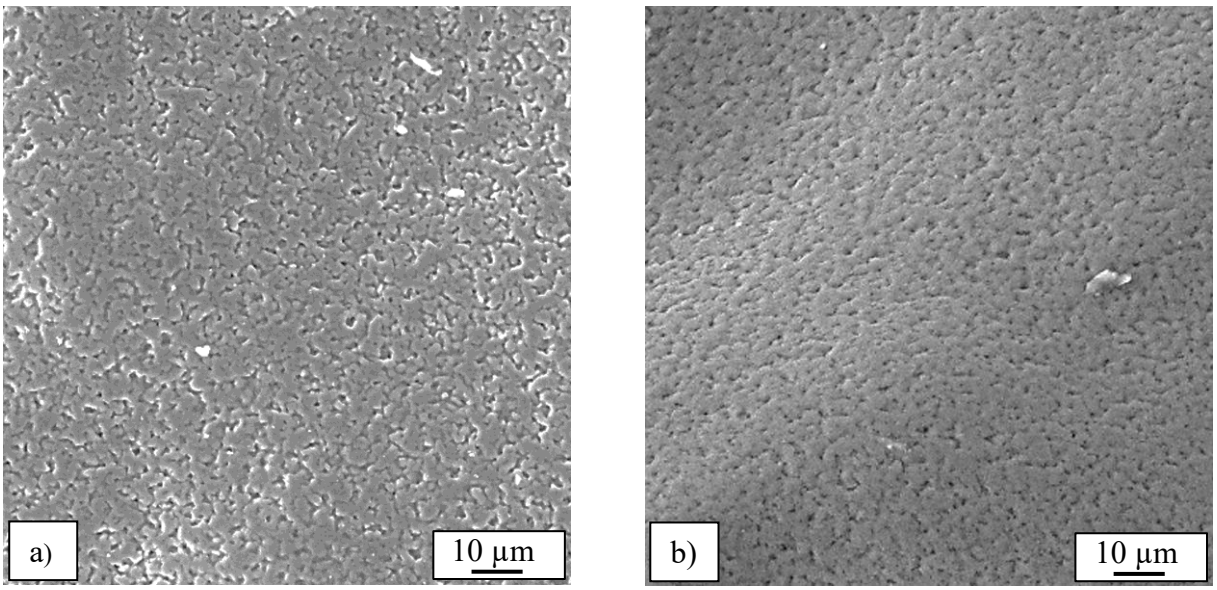

Figure 8. Secondary electron images of MAT effect material: a) Wall tile, b) Floor tile

3.4. Optical Properties

Figure 9 presents the surface gloss measurements of TRS, OPAK, and MAT effect materials applied to wall and floor tiles. The applications were carried out at coating weights of 25, 50, and 100 g/m². The gloss measurements of the tiles increased with the coating weight of TRS and OPAK effect materials, which is related to increased material coverage on the tile surface, resulting in a more uniform surface. The application temperature of the floor tile enables the effect material to spread efficiently across the surface. This analysis is supported by the SEM images of TRS and OPAK effect materials applied to wall and floor tile, as presented in Figures 5 and 6. The literature indicates that a glossy appearance is obtained through the smooth reflection of light beams on a flat surface. The intensity of the reflected beam affects the visual appearance of the surface. A glassy structure increases light reflection, producing a smooth and glossy finish, which enhances the aesthetic appearance and surface quality of the coated tiles. The gloss measurements of the MAT effect material on wall and floor tiles indicate that increasing the applied effect material has a limited impact on the

surface properties. Diffuse scattering of incoming light beams results in the matte appearance of a surface, primarily caused by the surface topography of glaze [26]. The higher softening point of the MAT effect materials results in a fine topography in the microstructures, which causes high diffuse reflection (Figures 8a and 8b). Increasing the amount of MAT effect material has an insignificant impact on gloss measurements due to the micro-rough texture formed on the surface, which scatters light subtly without significantly affecting the measurement of gloss.

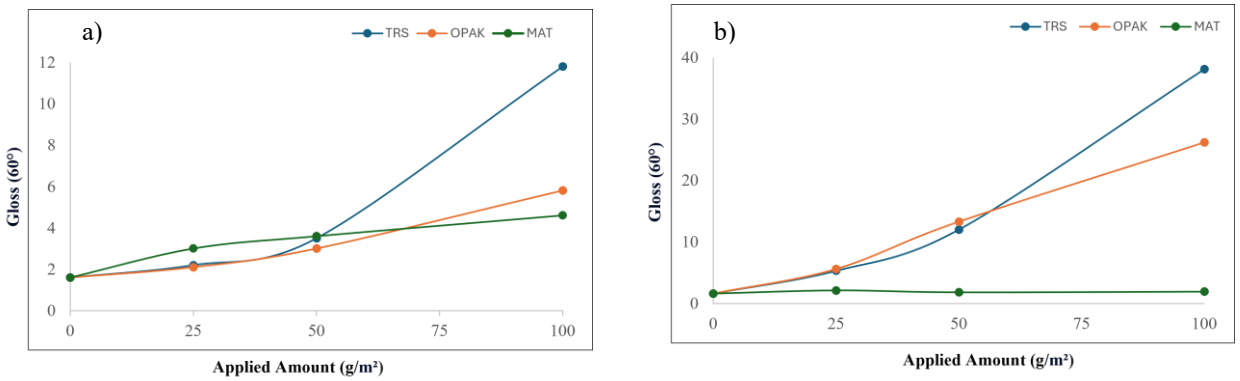

Figure 9. Surface gloss measurements of TRS, OPAK, and MAT effect materials as a function of increasing applied amount, a) Wall tiles, b) Floor tiles

4. Conclusion

This study demonstrated that frits with transparent, opaque, and matte surface properties are suitable as effect materials in industrial ceramic wall and floor tile applications through the high-energy ball milling process. The process achieved d_{90} values below 1.0 µm, preventing nozzle clogging, and maintained post-dilution viscosities within the optimal range of 15–25 mPa·s. The surface properties of coatings with different effect materials were also evaluated as a function of temperature. Coatings with TRS and OPAK effect materials showed an increase in gloss with rising temperature, resulting in smoother and more reflective surfaces. In contrast, coatings with the MAT effect material exhibited a fine and rough topography due to crystallization behavior. A high softening temperature combined with reduced viscous flow leads to restricted sintering and provides a matte surface appearance. In conclusion, variations in surface topography were identified as the key factor distinguishing matte from glossy surface finishes.

Author Contributions

The first and second authors performed data analysis and experiments. The first author wrote the paper. The second, third, and fourth authors reviewed and edited the paper. They all read and approved the final version of the paper.

Conflict of Interest

All the authors declare no conflict of interest.

Ethical Review and Approval

No approval from the Board of Ethics is required.

References

[1] J. Chen, B. He1, H. Zhu, J. Wu, *The implicit preference evaluation for the ceramic tiles with different visual features: Evidence from an event-related potential study*, Frontiers in Psychology 14 (2023) 1-13.

[2] I. Hutchings, *Ink-jet printing for the decoration of ceramic tiles: Technology and opportunities,* Proceedings of the World Congress on Ceramic Tile Quality, Castellón, 2010, 17 pages.

[3] G. Ferrari, P. Zannini, *Thermal behavior of vehicles and digital inks for inkjet decoration of ceramic tiles*, Thermochimica Acta 639 (2016) 41–46.

[4] M. Dondi, M. Blosi, D. Gardini, C. Zanelli, P. Zannini, *Ink technology for digital decoration of ceramic tiles: An overview,* Proceedings of the 13th World Congress on Ceramic Tile Quality, Castellón, 2014, 14 pages.

[5] T. Cao, Z. Yang, H. Zhang, Y. P. Wang, *Inkjet printing quality improvement research progress: A review*, Heliyon 10 (2024) e30163.

[6] C. Zanelli, G. L. Güngör, A. Kara, M. Blosi, D. Gardini, G. Guarini, M. Dondi, *Micronizing ceramic pigments for inkjet printing: Part II. Effect on phase composition and color*, Ceramics International 41 (2015) 6507–6517.

[7] H. Maleki, V. Bertola, *Recent advances and prospects of inkjet printing in heterogeneous catalysis,* Catalysis Science and Technology 10 (2020) 3140-3159

[8] J. H. Lee, J. W. Kweon, W. S. Cho, J. H. Kim, K. T. Hwang, *Formulation and characterization of black ceramic ink for a digital ink-jet printing,* Ceramics International 44 (2018) 14151–14157.

[9] C. Gao, T. Xing, X. Hou, G. Chen, *Preparation of disperse inks for direct inkjet printing of non-pretreated polyester fabrics,* RSC Advances 9 (2019) 9791-19799.

[10] E. Enriquez, J. J. Reinosa, V. Fuertes, J. F. Fernandez, *Advances and challenges of ceramic pigments for inkjet printing,* Ceramics International 48 (21) (2022) 31080–31101.

[11] C. Molinari, S. Conte, C. Zanelli, M. Ardit, G. Cruciani, M. Dondi, *Ceramic pigments and dyes beyond the inkjet revolution: From technological requirements to constraints in colorant design,* Ceramics International 46 (14) (2020) 21839-21872.

[12] O. Watanabe, T. Hibino, M. Sakakibara, *Development of an ink-jet printing system for ceramic tile,* Proceedings of the 12th World Congress on Ceramic Tile Quality, Castellón, 2012, 10 pages.

[13] B. Yazırlı, H. Sarı, K. Kayacı, F. Kara. *Effect of nucleating agent additions on gahnite-based glass-ceramic glazes.* Journal of the European Ceramic Society 44 (2024) 3344–3351.

[14] J. Partyka, J. Lis, *The influence of the grain size distribution of raw materials on the selected surface properties of sanitary glazes,* Ceramics International 37 (4) (2011) 1285-1292.

[15] R. Casasola, J. Ma Rincon, M. Romero, *Glass–ceramic glazes for ceramic tiles: A review,* Journal of Materials Science 47 (2012) 553-582.

[16] K. Pekkan, B. Karasu, *Zircon-free frits suitable for single fast-firing opaque wall tile glazes and their industrial productions,* Journal of the European Ceramic Society 29 (2009) 1571–1578.

[17] O. J. Akinribide, G. N. Mekgwe, S. O. Akinwamide, F. Gamaoun, C. Abeykoon, O. T. Johnson, P. A. Olubambi. *A review on optical properties and application of transparent ceramics,* Journal of Materials Research Technology 21 (2022) 712-738.

[18] M. Gajek, A. Rapacz-Kmita, E. Stodolak-Zych, M. Zarzecka-Napierała, M. Wilk, A. Magdziarz, M. Dudek. *Microstructure and mechanical properties of diopside and anorthite glazes with high abrasion resistance*, Ceramics International 48 (2022) 6792–6798.

[19] E. Bou, M. C. Bordes, C. Feliu, M. E. Gazulla, E. Ferrer, G. Pasies, *Variables that determine the matt appearance of some ceramic floor and wall tile glazes,* Proceedings of the 8th World Congress on Ceramic Tile Quality, Castellón, 2002, 16 pages.

[20] G. L. Güngör, A. Kara, D. Gardini, M. Blosi, M. Dondi, C. Zanelli, *Ink-jet printability of aqueous ceramic inks for digital decoration of ceramic tiles,* Dyes and Pigments 127 (2016) 148–154.

[21] I. N. Diaz, P. D. Corso*, Digital ceramic decoration, an introduction,* Asociacion Espanola Tecnicos Ceramicos (2017).

[22] D. Yazici, *Examining the relationship between the particle size distribution of frits used in ceramic tile production and their potential as effect materials,* Master's Thesis Eskişehir Technical University (2023) Eskişehir.

[23] D. Verucchi, M. Cavedoni, *Pigmented ceramic inks,* Ceramic World Review 91 (2011).

[24] P. M. T. Cavalcante, M. Dondi, G. Guarini, M. Raimondo, G. Baldi, *Color performance of ceramic nano pigments,* Dyes and Pigments 80 (2009) 226-232.

[25] D. Y. Park, S. J. Park, *Particle size-dependent viscosity behavior of a suspension using image processing,* Powder Technology 339 (2018) 686–694.

[26] D. R. Eppler, *Glazes and glass coatings,* American Ceramic Society, (2000).

[27] M. F. Gazulla, P. Gómez, A. Moreno, E. Bou, *Factors affecting frit solubility in glaze suspensions*, Boletín de la Sociedad Española de Cerámica y Vidrio 40 (2) (2001) 131–135.

[28] V. S. Solana, *Inkjet printing technology for ceramic tile decoration,* Proceedings of the 13th World Congress on Ceramic Tile Quality, Castellón, 2014, 15 pages.

[29] G. L. Güngör, A. Kara, M. Blosi, D. Gardini, G. Guarini, C. Zanelli, M. Dondi, *Micronizing ceramic pigments for inkjet printing: Grindability and particle size distribution.* Ceramics International 41 (2015) 6498–6506.